Membrane interactions of the hydrophobic segment of diacylglycerol kinase epsilon

ARTICLE *in* BIOCHIMICA ET BIOPHYSICA ACTA · NOVEMBER 2007

Impact Factor: 4.66 · DOI: 10.1016/j.bbamem.2007.06.012 · Source: PubMed

Available online at www.sciencedirect.com
ScienceDirect
Biochimica et Biophysica Acta 1768 (2007) 2549–2558
Biochimica et Biophysica Acta BBA
www.elsevier.com/locate/bbamem

Membrane interactions of the hydrophobic segment of diacylglycerol kinase epsilon

Evgenia Glukhov [a,b], Yulia V. Shulga [c], Raquel F. Epand [c], Armela O. Dicu [c], Matthew K. Topham [d], Charles M. Deber [a,b], Richard M. Epand [c,*]

[a] *Division of Molecular Structure & Function, Research Institute, Hospital for Sick Children, Toronto, Ontario, Canada M5G 1X8*
[b] *Department of Biochemistry, University of Toronto, Toronto, Ontario, Canada M5S 1A8*
[c] *Department of Biochemistry and Biomedical Sciences, McMaster University Health Science Center, Hamilton, Ontario, Canada L8N 3Z5*
[d] *Huntsman Cancer Institute, University of Utah, Salt Lake City, UT 84112, USA*

Received 26 April 2007; received in revised form 26 May 2007; accepted 12 June 2007
Available online 21 June 2007

Abstract

Diacylglycerol kinase epsilon (DGKε) is unique among mammalian DGK isoforms in having a segment of hydrophobic amino acids as a putative membrane anchor. To model the conformation, and stoichiometry of this segment in membrane-mimetic environments, we have prepared a peptide corresponding to this hydrophobic segment of DGKε of sequence KKKKLILWTLCSVLLPVFITFWKKKKK-NH_2. Flanking Lys residues mimic the natural setting of this peptide in DGKε, while facilitating peptide synthesis and characterization. Circular dichroism and fluorescence spectroscopic analysis demonstrated that the peptide has increased helical content and significant blue shifts in the presence of anionic – but not zwitterionic – bilayer membranes. When labeled with fluorophores that can undergo fluorescence resonance energy transfer, the peptide was found to dimerize – a result also observed from migration rates on SDS-PAGE gels under both reducing and non-reducing disulfide bridge conditions. The peptide was shown to preferentially interact with cholesterol in lipid films comprised of homogeneous mixtures of cholesterol and phosphatidylcholine, yet the presence of cholesterol in hydrated vesicle bilayers decreases its helical content. The peptide was also able to inhibit the activity of DGKε protein *in vitro*. Our overall findings suggest that the peptide ultimately cannot leave the bulk water for attachment/insertion into the outer leaflet of an erythrocyte-like bilayer, yet its core sequence is sufficiently hydrophobic to insert into membrane core regions when membrane attachment is promoted by electrostatic attraction to anionic lipid head groups of the inner leaflet of an erythrocyte-like bilayer.

Keywords: Diacylglycerol kinase; Hydrophobic segment; Transmembrane helix; Membrane protein oligomerization

1. Introduction

The mammalian DGK family is comprised of ten isoforms, of which nine have been identified and studied extensively [1], while the tenth one has been identified recently [2]. All mammalian DGK isoforms have a conserved catalytic domain responsible for kinase activity. In addition, all DGKs have at least two cysteine-rich regions that are predicted to bind diacylglycerol (DAG). Most DGKs have other structural domains that likely have regulatory roles and which separate the isoforms into five families [2–6]. One distinct class of mammalian DGKs, the type III, appears to have no other regulatory domains apart from the Cys-rich regions (C1 domains) and the catalytic domain. DGKε is the only known type III isoform. The biological importance of DGKε in neuronal function has been demonstrated in studies with knock-out mice [7–9]. DGKε is a 64-kDa protein which is unique in having a preference for DAG substrates with an arachidonate moiety [10]. DGKε is also unique in being the only DGK isoform with a predicted transmembrane

Abbreviations: CD, circular dichroism; DAG, diacylglycerol; DGK, diacylglycerol kinase; DGKε, epsilon isoform of DGK; DGKζ, zeta isoform of DGK; DMPS, 1,2-dimyristoylphosphatidylserine; DSC, differential scanning calorimetry; SAG, 1-stearoyl-2-arachidonoyl glycerol; DOG, 1,2-dioleoyl glycerol; DOPC, 1,2-dioleoylphosphatidylcholine; FRET, fluorescence resonance energy transfer; L22W39-K_9, KKKKLILWTLCSVLLPVFITFWKK-KKK-NH_2; LPC, lysophosphatidylcholine; OG, octyl glucoside; MRE, mean residue ellipticity; PA, phosphatidic acid; POPC, 1-palmitoyl-2-oleoylphosphatidylcholine; SOPC, 1-stearoyl-2-oleoylphosphatidylcholine; SUV, small unilamellar vesicle; TDW, triply distilled water; TM, transmembrane

* Corresponding author. Tel.: +1 905 525 9140x22073; fax: +1 905 521 1397.
E-mail address: epand@mcmaster.ca (R.M. Epand).

0005-2736/$ - see front matter © 2007 Elsevier B.V. All rights reserved.
doi:10.1016/j.bbamem.2007.06.012

Table 1
Segments in DGKε identified as putative transmembrane helices

Species	Residues	Sequence
Human	21–41	LILWTLCSVLLPVFITFWCSL
Monkey	21–41	LILWTLCSVLLPVFITFWCSL
Rat	19–39	LILWTLFSVLLPVFITLWCSL
Mouse	19–39	LVLWTLCSVLLPVFITLWCSL
Drosophila	16–36	LLALSILFAFCRSLLSEDFVS
Arabidopsis thaliana (DGK2)	20–40	FIFGWLVTGSVGLLAVIYTFL

(TM) helix [11]. This putative TM comprises approximately residues 20–40 and is found in all forms of mammalian DGKε, as well as in *Drosophila* and in DGK2 from *Arabidopsis thaliana* (Table 1). Interestingly, DGK2 has also been found to exhibit specificity for DAG substrates with arachidonic acid [12]. Studies on known tail-anchored proteins have similarly indicated the requirement for the suitable length of helical structure of the α-helical TM segment, along with multiple positive charges in the C-terminal region adjacent to the TM – often within five residues – as critical for targeting to mammalian mitochondria [13].

The hydrophobic segment of a membrane protein can have several roles including sequestering the protein to a membrane, determining the topology of the protein in a membrane and preferentially interacting with other components of the membrane, both lipid and protein. The present study investigates the abilities of a model peptide corresponding to the predicted TM sequence of DGKε to interact with membrane components, using circular dichroism, tryptophan fluorescence, and FRET; to inhibit DGK activity [14]; and to interact with cholesterol in membrane bilayers. The results provide insights into the functional importance of this segment in intact DGKε.

2. Materials and methods

2.1. Modeling

The *TM Finder* program [15] with default settings of N-terminal window size, C-terminal window size, minimum core length, closed-gap length, and minimum segment length was applied to total primary sequences of DGKε from different species in order to identify potential TM sequences. The *TM Finder* program accepts the primary sequence in FASTA format as input, and generates a dual hydropathy/helicity plot as a function of protein primary sequence. The helical wheel for the L22–W39 sequence was built by the wheel.pl program (http://rzlab.ucr.edu/scripts/wheel/wheel.cgi) [16]. Energy-minimized models of the interaction between two idealized helices were produced using a global conformation search program CHI as described [17].

2.2. Reagents

Reagents for peptide synthesis, cleavage, and purification included 9-fluorenylmethoxy carbonyl (Fmoc)-protected amino acids (Novabiochem); Fmoc-PAL-PEG-PS-resin, piperidine (Applied Biosystems, Foster City, CA); *N*,*N*-dimethylformamide (DMF), methanol, diethyl ether, acetonitrile (Caledon Laboratories Ltd., Georgetown, Ontario, Canada); *N*,*N*-diisopropylethylamine (DIEA; Aldrich); *O*-(7-azabenzotriazol-1-yl)-1,1,3,3-tetramethyluronium hexafluorophosphate (HATU; GL Biochem Ltd., Shanghai, China). Buffer was prepared using Tris sodium salt in doubly distilled water with adjustment to pH=7.0 by HCl. Lipids LPC, POPC and DMPS were purchased from Avanti Polar Lipids (Alabaster, AL). Fluorescent probes (dansyl- and dabcyl-chlorides) are from Molecular Probes (Eugene, OR); NuPAGE gels and NuPAGE SDS sample buffer from Novex (San Diego, CA). Histone HI was from GIBCO/BRL (Grand Island, NY); ATP was the disodium salt, SigmaUltra grade (Sigma, St. Louis, MO). [γ-^{32}P] ATP was from Perkin Elmer (Boston, MA). All chemicals were used without further purification.

2.3. Peptide synthesis

The DGKε transmembrane domain peptide L22W39-K_9 was synthesized by standard solid-phase protocols using Fmoc chemistry on a PerSeptive Biosystems Pioneer peptide synthesizer as described [18,19]. Following a standard cleavage procedure (89% TFA, 4.5% phenol, 4.5% TDW, 2% triisopropylsilane), crude peptide was precipitated in cold ethyl ether and purified on a reverse-phase C18 high performance liquid chromatography column (Vydac, 250×21.5 mm) using a linear gradient 20–80% B (Buffer A: 0.1% TFA, 95% TDW, 5% AcCN; Buffer B: 0.1% TFA, 95% AcCN, 5% TDW) for the 60 min. Molecular masses were confirmed by MALDI mass spectrometry. Peptide concentrations were determined in triplicate by standard bis-cinchinonic acid assay. Peptide solutions were stored at −20 °C and used with 5% (v/v) of beta-mercaptoethanol where reducing conditions were required.

2.4. SDS-PAGE gel electrophoresis

Peptide samples were subjected to SDS-PAGE, using NuPage pre-cast 12% Bis-Tris gels (1.0 mm×10 well). L22W39-K_9 was dissolved in sample buffer (with or without beta-mercaptoethanol) prior to electrophoretic separation at 125 mV. The $MW_{exp.}$:$MW_{theor.}$ ratios were calculated from each stained gel using See blue marker and the NIH 1.62 Image Program, software available at http://www-cellbio.med.unc.edu/henson_mrm/pages/NIH.html [20].

2.5. Preparation of phospholipid small unilamellar vesicles (SUVs)

SUVs were prepared using standard procedures as described previously [21]. The desired amount of lipids in chloroform was dried in glass tubes under nitrogen, and lyophilized overnight to obtain lipid films that were suspended for 1 h in a water-bath at room temperature in Tris–HCl buffer, while sealed with parafilm under nitrogen. Sonication of lipid dispersions was performed in 5 mL glass tubes in a bath-type sonicator (G112SP1G, Laboratory Supplies Co., Hicksville, NY) for 5 min (until clear). To avoid degradation of unsaturated lipids, sonication was performed at ~10 °C under a nitrogen atmosphere. Vesicles were used on the day of preparation.

2.6. Circular dichroism (CD) spectroscopy

Circular dichroism spectra were collected using a Jasco J-720 spectropolarimeter. Spectral scans were performed from 250 to 195 nm, with step resolution of 0.1 nm and bandwidth of 1.0 nm at a speed 50 nm/min [22]. A 1-mm-path-length quartz cuvette was used for the measurements and values from 3 scans were averaged and corrected for noise. Freshly prepared samples were measured at L22W39-K_9 concentration of 30 μM. Aqueous buffer containing 10 mM Tris–HCl, 10 mM NaCl at pH=7.0 was used as a solvent for measurements and its background (in presence of appropriate detergents and salts where required) was subtracted for each sample. For SUVs samples of zwitterionic (POPC) or anionic (POPC:DMPS=9:1) lipids in presence or absence of 30% cholesterol were sonicated in presence of the peptide or alternatively vesicles were first prepared and peptide was added subsequently, and the sample allowed to equilibrate for 10 min. The spectra are reported as mean residue molar ellipticity ($[\theta_n]$, ° cm^2 dmol^{-1}) that were calculated with CDpro software

$$[\theta_n] = [\theta_n]_{observed} * (MRW/10lc) \quad (1)$$

where $[\theta_n]_{observed}$ is the ellipticity measured, MRW is mean residue molecular mass taken as 110, l is optical path length of the cell in cm and c is peptide concentration in μM.

The helical content was estimated according to the Chen et al. [23] as:

$$[\theta_n]_{222} = -39500 * (1 - 2.57/n) \quad (2)$$

where n=number of residues.

2.7. Fluorescence measurements

Fluorescence emission spectra of L22W39-K_9 Trp residues and FRET were recorded on a Hitachi F-400 Photon Technology International C-60 fluorescence spectrometer. For Trp fluorescence, semimicro quartz cuvettes of 0.5 mL (10 mm excitation path length and 4 mm emission path length) (Hellma, Concord, ON) were used. Excitation wavelength was 280 nm, and emission spectra were recorded from 305 to 395 nm. Spectra were collected with a step size of 1 nm with averaging of two cycles. Excitation and emission slit widths were 2 and 4 nm, respectively. All measurements were corrected for light scattering effects by subtraction of background and by the correction function of the manufacturer's software. Background samples were prepared using the same protocol except pure water instead of peptide solution was added. Blue shifts were calculated as the difference in wavelength of the maxima in emission spectra of lipid–peptide and normal ionic strength aqueous peptide samples. 4 μM peptides were used in 1 mM total lipid concentration, a lipid-to-peptide ratio of 250 was established.

2.8. FRET measurements

Labeling of L22W39-K_9 was achieved by coupling of dansyl or dabcyl chlorides to its N-terminal Lys [24]. Samples were titrated at room temperature at constant stirring in a stoppered 10 mm × 10 mm disposable cuvettes. Emission spectra were collected from 450 nm to 650 nm, λ_{ex} = 341 nm, 0.5 s/nm, band pass was 4 nm for both excitation and emission. Peptides were diluted in buffer (10 mM Tris–HCl, 10 mM NaCl, pH = 7.0, with 5% v/v beta-mercaptoethanol) with either 25 mM SDS detergent or 1 mM SUVs. The concentration of dansyl-labeled L22W39-K_9 was kept constant at 1 μM, and the total concentration of dansyl-, dabcyl- and unlabeled peptides was kept constant at 5 μM. Each mixture was allowed to equilibrate for 3 min. Each spectrum is the average of two runs.

2.9. DGK activity assay in OG micelles

For DGKε assays lipid films were prepared using SAG as a substrate mixed with DOPC in 2:1 $CHCl_3/CH_3OH$, with or without the addition of L22W39-K_9 in CH_3OH. The solvent was then evaporated under a stream of nitrogen with constant rotation of a test tube so as to deposit a uniform film of lipid over the bottom third of the tube. Last traces of solvent were removed by placing the tube under high vacuum for at least 2 h. The micelles were prepared by adding of 50 μL of 4X assay buffer (300 mM OG, 400 mM NaCl, 20 mM $MgCl_2$, 4 mM EGTA, 200 mM MOPS, pH 7.2) and thorough vortexing for 2 min. The final reaction mixture contained 50 μL of micelles, 20 μL of 10 mM DTT, 20 μL of 100 mM $CaCl_2$, 10 μL of cell lysate from cells infected with Baculovirus stocks containing DGKε cloned into BacPAK6 and carrying a C-terminus 6XHis epitope, and ddH_2O to 180 μL. The reaction was initiated by adding 20 μL of 5.0 mM [γ-^{32}P] ATP (50 μCi/mL) and incubated for 10 min at 25 °C. The concentrations of SAG, DOPC and the peptide in the final volume (200 μL) were 0.24 mM, 4.5 mM and 0.13 mM, respectively. To terminate the reaction, 2 mL of $CHCl_3/CH_3OH$ (1:1 v/v) containing 0.25 mg/mL dihexadecyl phosphate was added. The organic phase was washed three times with 2 mL of 1% $HClO_4$, 0.1% H_3PO_4 in CH_3OH/H_2O (7:1 v/v). A 0.4-mL aliquot of the organic phase was used to determine the incorporation of ^{32}P into PA by Cerenkov counting. Controls were run without the addition of cell lysate. The assays were done in triplicate and the results are presented as mean ± the standard deviation for each experiment.

DGKζ assays were performed as for DGKε with the following differences: lipid films were prepared using 1,2-DOG as a substrate, DOPS (in 2:1 $CHCl_3/CH_3OH$) and with/without addition of the peptide (in CH_3OH). The final reaction mixture contained 50 μL of micelles, 20 μL of 10 mM DTT, 20 μL of cell lysate and ddH_2O to 180 μL. The concentrations of DOG, DOPS and the peptide in the final volume (200 μL) were 0.8 mM, 5 mM and 0.13 mM, respectively.

2.10. Differential scanning calorimetry (DSC)

Lipid films with or without L22W39-K_9 were prepared as described above for the DGK assays. The lipid film was then hydrated with 20 mM PIPES, 1 mM EDTA, 150 mM NaCl with 0.002% NaN_3, pH 7.40 and suspended by intermittent vortexing and heating to 50 °C over a period of 2 min under argon. DSC measurements were made using a Nano Differential Scanning Calorimeter (Calorimetry Sciences Corporation, Lindon, UT). The scan rate was 2 °C/min and there was a delay of 5 min between sequential scans in a series to allow for thermal equilibration. The features of the design of this instrument have been described [25]. DSC curves were analyzed by using the fitting program, DA-2, provided by Microcal Inc. (Northampton, MA) and plotted with Origin, version 5.

3. Results

3.1. Peptide design and secondary structure

Several algorithms for predicting TM helices identify a segment in all known forms of DGKε from various species, including the arachidonoyl-specific DGK2 from *A. thaliana*, centered around N-terminal residues 20–40 as being a putative α-helical TM segment (Table 1). The segment is well conserved among mammalian DGKε species. These methods include *TM Finder* (www.bioinformatics-canada.org/TM/) [15], which is based on the dual requirements of hydrophobicity and membrane helical propensity, along with IMPALA [26] and DAS [27]. The predicted TM domain of human DGKε is located at the N-terminal region of the protein sequence, where the first 47 residues are M^{1}EAERRPAPGSPSEGLFADGH-**L^{22}ILWTLCSVLLPVFITFW^{39}**-CSLQRSRR^{47}. The predicted membrane-spanning domain L22–W39 is shown in bold, while flanking positively charged residues are underlined. A polar His residue is also present at the N-terminus of the putative TM segment. This potential TM segment has significant hydrophobicity, four aromatic residues (known as efficient promoters of partitioning into membranes [28]) and flanking positive charges within four residues of the C-terminal TM region. The average hydrophobicity [14] of this segment of DGKε is significantly above that of many well-researched integral membrane proteins, such as the influenza hemagglutinin [29]. As positively charged amino acids tend to be more prevalent on the cytoplasmic than on the extra-cytoplasmic side of TM proteins [30], localization of three Arg residues downstream of the L22–W39 segment support the hypothesis that it serves as an cell membrane anchor of the protein. In this context, a model peptide was designed to correspond to the TM segment of the human DGKε sequence L22–W39 while incorporating terminally-located positive character. The L22–W39 has a segmental core hydrophobicity of 2.8 on the Liu–Deber scale [15,22], a value above the fundamental hydrophobicity threshold for membrane insertion (0.4) into micelles and anionic cell membranes. According to 'Lys-tagging' guidelines for synthesis of hydrophobic peptides [24], a total of nine Lys residues were attached to the hydrophobic core sequence of L22–W39 to produce an initial water-soluble product. The resulting peptide, designated L22W39-K_9, has sequence KKKK-LILWTLCSVL-LPVFITFW-KKKKK-NH_2. Consistent with previous applications of this hydrophilic tagging approach, we found that the peptide designed in this manner had the beneficial attributes of water solubility and ease of purification [31,32]. Attachment of multiple Lys residues to the both termini of TM L22–W39 domain mimics the presence of three neighboring positively charged Arg (and an N-terminal His residue) both upstream and downstream from the native sequence.

3.2. Helicity of the DGKε TM domain peptide in membrane environments

The secondary structure of the DGKε TM domain peptide was found to be medium-dependent. Thus, L22W39-K_9 is largely in a random coil conformation in aqueous buffer (Fig. 1A) as measured by CD spectroscopy. *TM Finder* data analysis [15] predicts that the L22–W39 core segment will adopt an α-helical structure in membrane-mimetic environments. Consistent with this L22W39-K_9 displayed the ability to spontaneously insert into anionic SDS micelles where it adopts a high degree of helicity, the mean residue ellipticity at 222 nm is −24,000° cm^2 $dmol^{-1}$ (Fig. 1A), corresponding to *ca.* 18 peptide residues as helical [23] (the full hydrophobic core)—in principle a sufficient length for a protein transmembrane segment [33]. Although CD spectra obtained in presence of zwitterionic LPC micelles (Fig. 1A) show some partial helicity (mean residue ellipticity of −10,000° cm^2 $dmol^{-1}$ at 222 nm), typical random coil profile spectra in zwitterionic SUVs prepared from POPC (model of the outer leaflet of a plasma membrane [34]) in the presence or absence of cholesterol, were indicative of a lack of peptide insertion (Fig. 1B). In contrast, in anionic SUVs (PC:PS=9:1) in the presence of 30% cholesterol (a lipid mixture typical of the inner leaflet of a mammalian plasma membrane [34]) (Fig. 1B), the peptide showed some characteristic α-helix folding with a moderate degree of helicity −7000° cm^2 $dmol^{-1}$—that is similar to that observed in the presence of zwitterionic micelles. A more significant helicity level – up to −12,000° cm^2 $dmol^{-1}$ (equivalent to ca. 10 residues) – was observed in the same anionic SUVs in the absence of cholesterol (Fig. 1B). Interestingly, in the latter experiments with SUVs, no difference was observed whether the peptide was added before or after the sonication process for vesicle formation (Fig. 1C).

3.3. Membrane insertion of the DGKε TM domain studied by fluorescence spectroscopy

Measurements of fluorescence emission intensity and shifts in the λ_{max} of two Trp residues naturally contained in the hydrophobic core of the peptide are particularly useful for analysis of the insertion/positioning of L22W39-K_9 within the membrane [35]. Thus, we exposed the peptide to SDS micelles, and to freshly prepared zwitterionic SUV-POPC and anionic SUV-POPC:DMPS/9:1 at 250:1 lipid-to-peptide molar ratio in both cases. In the experiments with SDS micelles and anionic lipid-containing vesicles, the peptide displayed similar significant blue shifts of $\Delta\lambda_{max}$=20 nm or 18–19 nm, respectively (Table 2), accompanied by spectral intensity enhancement. These results provide evidence of insertion of the peptide into non-polar environments [35]. In contrast, negligible shifts in either maximum wavelength or intrinsic fluorescence intensity were seen in the presence of zwitterionic vesicles mimicking the

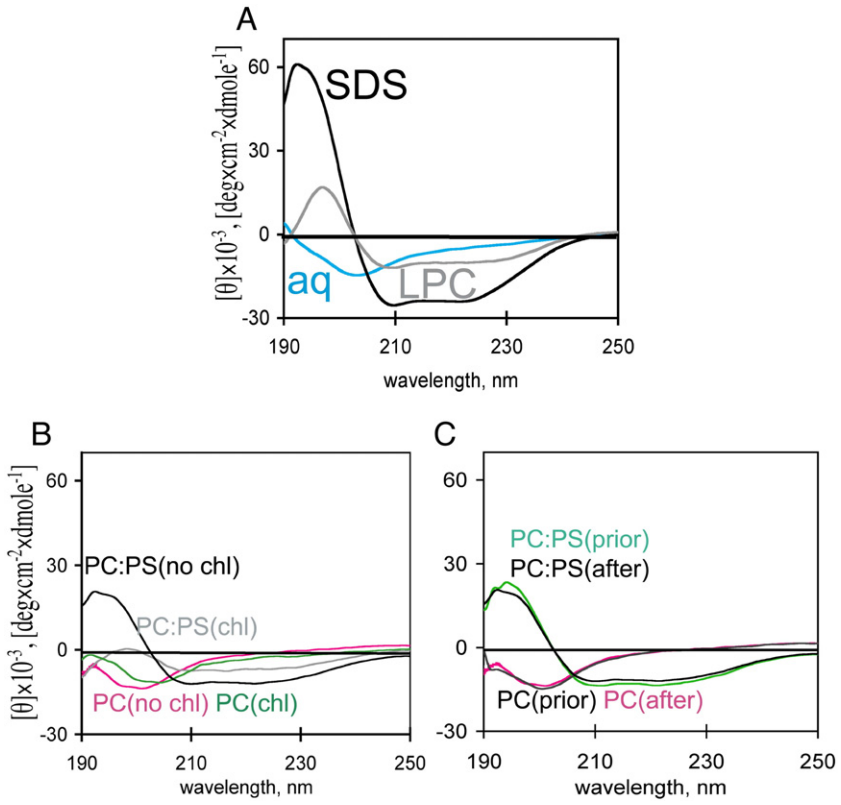

Fig. 1. Circular dichroism spectra of L22W39-K_9 recorded in various media, as indicated on the diagram. (A) Aqueous buffer; LPC micelles; and SDS micelles; (B) anionic SUV-POPC:DMPS=9:1 in presence or absence of 30% cholesterol; zwitterionic SUV-POPC vesicles in presence or absence of 30% cholesterol; (C) anionic SUV-POPC: DMPS=9:1, with peptide added prior to, or after, sonication; zwitterionic POPC SUV vesicles, with peptide added prior to, or after, sonication.

Table 2
Emission maxima shifts ($\Delta\lambda_{max}$) of L22W39-K_9 relative to the λ_{max} values in aqueous media

Medium	$\Delta\lambda_{max}$, blue shift, nm [a]
SDS [b]	20
SUV-PC [b]	4.0
SUV-PC:PS [b]	18
High salt [c]	11

[a] These values are relative to the observed emission maximum in water at low salt concentration of 348 nm. Estimated uncertainty in $\Delta\lambda_{max}$ values, ±1 nm.
[b] [NaCl]=10 mM.
[c] [NaCl]=1.5 M.

external leaflet (Table 2). The shifts from peptides added to the pre- and post-vesicle formation were identical.

3.4. Evidence for oligomerization of the DGKε TM peptide

The peptide L22W39-K_9 contains a Cys residue that can form disulfide bridged intermolecular dimers. However, SDS-PAGE electrophoresis of the peptide at 30 μM demonstrated that in both reducing and non-reducing conditions, the peptide forms dimers (MWexp/MWtheor=1.9±0.2) and trimers (MWexp/MWtheor=2.7±0.2), indicating that the peptide has a strong tendency to oligomerize through non-covalent interactions that are resistant to SDS denaturation (Fig. 2). At low peptide concentrations (silver staining, 1 μM) under non-reducing conditions, monomer (MWexp/MWtheor=1.1±0.2) as well as dimeric and trimeric forms, were observed (not shown), indicating that the peptide undergoes concentration-dependent oligomerization. The dimeric band was the strongest one in all experiments. On PFO-PAGE gels, L22W39-K_9 was highly aggregated (not shown).

Quenching of donor (N-terminal dansyl labeled peptide) fluorescence as a function of the acceptor (N-terminal dabcyl labeled peptide) fraction, as a result of FRET, can be used to determine the stoichiometry of association in peptide oligomers [24,36,37]. If the peptide remains monomeric, no quenching should be observed; if oligomerization occurs, the relative quantum yield of the donor decreases linearly in the case of dimerization, or according to a more complex function upon higher order oligomer formation [38]. In order to further evaluate the process of L22W39-K_9 oligomerization in membranes, FRET experiments were performed under reducing conditions in the presence of anionic micelles and anionic vesicles with acceptor. Since comparable results were obtained with peptides added prior to and after sonication (see Sections 3.2 and 3.3), titrations could readily be performed in the SUV environment. We confirmed the high tendency of the L22W39-K_9 peptide toward dimerization in both environments, where quenching vs. the mole fraction of dabcyl acceptor gave essentially linear relationships with significant slope values (−0.2 in SDS and −0.4 in anionic SUVs) (Fig. 3).

As an additional test of the tendency of this peptide toward self-association in solution, the peptide fluorescence was measured under high salt conditions [39]. The resulting blue shift of $\Delta\lambda_{max}$=11±1.4 nm in Trp fluorescence emission maximum (Table 2) indicates an increase in the hydrophobicity level of the environment of the Trp residues at high ionic strength, suggesting a degree of aggregation or oligomerization of the peptide under these conditions.

3.5. Effect of L22W39-K_9 on the activity of DGKε and DGKζ

DGKε and DGKζ activity assays were performed in the presence and absence of L22W39-K_9. The results showed the inhibition effect of L22W39-K_9 on both DGKε and DGKζ activities (Fig. 4). The peptide decreases DGKε activity by 43% (from 0.138 nmol/min to 0.0788 nmol/min), and DGKζ activity by 38% (from 0.0052 to 0.0032 nmol/min). The assay with DGKε was performed using the more specific substrate SAG, while that for DGKζ was performed with DOG as substrate and with the addition of DOPS required for higher activity of this isoform.

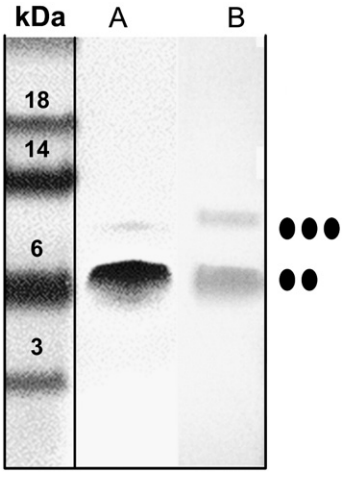

Fig. 2. Nu-PAGE electrophoresis of 2 μg L22W39-K_9 peptide under (A) Nonreducing conditions; and (B) reducing conditions (in presence of 5%(v/v) β-mercaptoethanol). Two dots represent the position of a dimer band, three dots represent a trimer band.

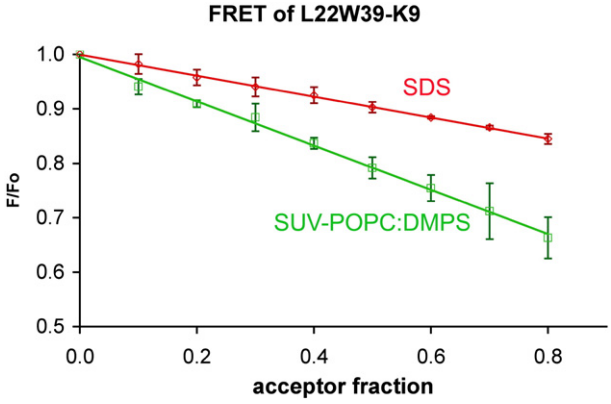

Fig. 3. FRET analysis of L22W39-K_9 dimerization in SDS micelles (red diamonds) and SUV- POPC:DMPS/9:1 (green squares). Dots represent fluorescence signals from dabcyl-labeled L22W39-K_9 titrated into a mixture of dansyl-labeled and unlabeled L22W39-K_9. F=fluorescence at any point; F_0=fluorescence in the absence of acceptor.

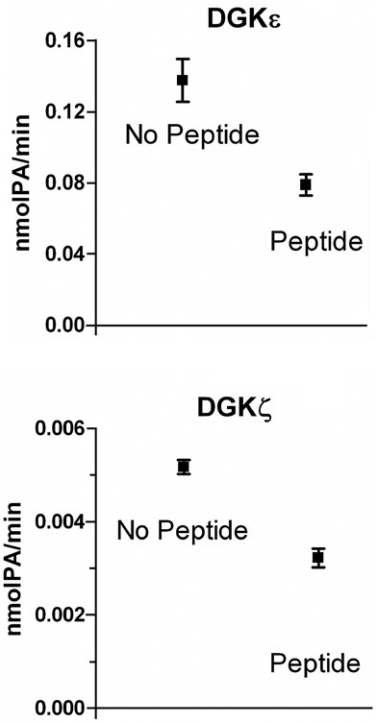

Fig. 4. Comparison of the activities of DGKε and DGKζ in the presence and absence of L22W39-K_9. DGKε, dark grey bars; DGKζ, light grey bars. See Materials and methods for further details.

3.6. L22W39-K_9 facilitates the formation of cholesterol-rich domains

Proteins play an important role in the distribution of cholesterol in membranes [40] as a consequence of cholesterol being either enriched or depleted from the environment of the protein. The peptide-induced changes in the lateral distribution of cholesterol in membranes can be assessed by determining the effect of cholesterol in broadening and lowering the enthalpy of the phase transition of phosphatidylcholine [41]. Addition of 10 mol% L22W39-K_9 to mixtures of SOPC with varying mole fractions of cholesterol results in the chain melting transition of SOPC increasing in enthalpy, indicative of the depletion of cholesterol from a region of the membrane (Table 3, Fig. 5). There is also the appearance of a transition with the characteristics of the polymorphic transition of anhydrous cholesterol crystals [42], suggesting that cholesterol exceeds its solubility limit in regions of the membrane in which it is enriched. This transition also exhibits a characteristic hysteresis [43], confirming its assignment as the polymorphic transition of anhydrous cholesterol crystals. The peptide also lowers the transition enthalpy of pure SOPC, unlike less hydrophobic peptides that exhibit greater preferential interaction only with membranes containing cholesterol [44].

Table 3
Enthalpy of phase transitions of mixtures of SOPC and cholesterol

% Cholesterol	Enthalpy of SOPC transition (kcal/mol SOPC)[a]		Enthalpy of anhydrous cholesterol crystals (cal/mol cholesterol)[b]
	Pure lipid	+10% L22W39-K_9	
0	4.0	3.0	0
30	0.50	0.63	0
40	0.1	0.60	70
50	>0.1	Not determined[c]	140

[a] Enthalpies are the average of heating and cooling scans.
[b] The enthalpy of anhydrous cholesterol crystals is measured in the presence of peptide. No such transitions are observed for the pure lipid mixtures. The transition enthalpy for pure anhydrous cholesterol crystals is 910 cal/mol [41].
[c] Transition too broad to obtain an accurate value.

4. Discussion

4.1. Membrane insertion of L22W39-K_9

All isoforms of DGK must access the cell membrane to act on the lipid substrate DAG. However, since DGKε is unique

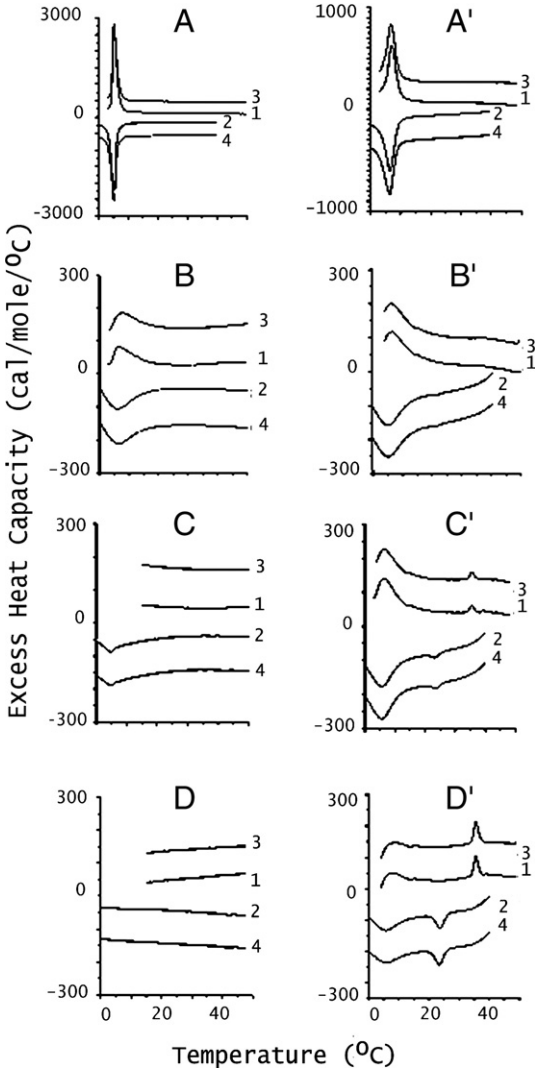

Fig. 5. Differential scanning calorimetry of SOPC with (A' to D') and without (A to D) 10 mol% L22W39-K_9 mixed with SOPC containing 0 (A and A'), 30 (B and B'), 40 (C and C') or 50 (D and D') mol% :cholesterol. Scan rate 2 K/min. Lipid concentration 2.5 mg/mL in 20 mM PIPES, 1 mM EDTA, 150 mM NaCl with 0.002% NaN3, pH 7.40. Sequential heating and cooling scans shown between 0 and 50 °C. Numbers are the order in which the scans were carried out, with scans 1, 3 and 5 being heating scans, each of which was followed by one of the cooling scans 2, 4 or 6. Scans were displaced along the y-axis for clarity of presentation.

among the 10 isoforms of this enzyme found in mammals in having a segment of hydrophobic residues that could function as a TM helix, DGKε may be the only DGK isoform that is permanently associated with the membrane. We sought to determine how this segment, recognized *in silico* as the L22–W39 sequence of human DGKε, can by itself contribute to determining the properties of the intact protein and its interactions with the cell membrane. One likely role is that the hydrophobic segment increases the partitioning of the enzyme to a cell membrane. To act as an anchor, the sequence corresponding to the potential TM segment, should insert spontaneously into the membrane bilayer and either traverse the membrane to form a transmembrane helix, or adopt a membrane-buried disposition below the bilayer surface but within one monolayer.

The designed L22W39-K_9 peptide served as a model of putative DGKε TM segment. As a contiguous sequence of 18 hydrophobic residues, the core of L22W39-K_9 is theoretically suitable for a membrane-spanning domain [33]. As well, blue shifts in Trp emission spectra and conformation transitions toward ordered structure observed in our experiments in the presence of cell membrane lipid preparations are typical evidence of peptide insertion *per se*. Although by the criterion of CD spectra, the L22W39-K_9 peptide is only partially helical, displaying modest helicity in anionic SUVs in absence of cholesterol and in zwitterionic LPC preparations, it displays significant helicity in SDS micelles, reaching a helical content of the requisite 18 residues (Fig. 1A, B). Consistent with CD findings, when monitored by Trp fluorescence shifts, the peptide does not insert into zwitterionic SUVs, but spontaneously inserts into anionic SUVs and SDS micelles (Table 2). As established by the observed decrease in helicity level, the presence of cholesterol in significant proportions seems to mitigate against the L22W39-K_9 insertion into anionic bilayers. Overall, the largely helical structure of L22W39-K_9 provides experimental confirmation that this sequence can readily insert into membrane environments, and as such, could potentially exist *in vivo* as a bona fide TM segment anchoring DGKε to the cellular membrane. Nevertheless, our finding of moderate helicity levels and fluorescence blue shifts of L22W39-K_9 in anionic phospholipid vesicles allows an alternative description for the mode of insertion of this peptide into membranes. Thus, the results do not rule out a topology of the peptide that is less deeply inserted into the non-polar regions of the membrane as a consequence of the presence of a kink near Pro-33 that could promote a 'cis-like' disposition of the peptide *vis-à-vis* the membrane. It can be noted that another hydrophobic peptide, pardaxin, also forms a kink at a Pro residue and is only partially helical in a membrane [45]. This peptide also promotes the formation of cholesterol-rich domains [46].

In the DSC studies, the peptide was added to the solution of lipid in organic solvent prior to hydration. This procedure is different from that used for CD experiments, where the peptide is added to preformed vesicles in buffer. This may explain why the presence of a large proportion of neutral cholesterol lipids in a bilayer is also able to interfere with membrane insertion of the peptide, as signaled in CD spectra by the decrease in its α-helical content upon cholesterol addition (Fig. 1B) although by DSC it is shown that the peptide can interact with cholesterol-containing membranes when initially mixed in organic solvent.

4.2. Dimerization tendency of L22W39-K_9

Once membrane-bound, the DGKε TM domain likely forms dimers and trimers, as shown by SDS-PAGE and FRET experiments (Figs. 2 and 3) even at low concentrations and under reducing conditions. These observations must also be considered in any model for the mode of function of this protein. The predicted peptide TM sequence contains neither charged side chains to form intermolecular ionic bonds [47,48], nor any "small" residue-xxx-"small" residue dimerization motifs such as GxxxG or AxxxA, arguing against these well-established modes of self-interaction of TM helices [32,49]. However, the TM sequence does contain a canonical leucine zipper motif characterized by general formula of **a**bc**d**efg, where **a** and **d** [50,51] can contribute to van der Waals association of helices [52], while multiple weakly polar residues can drive their strong association through the formation of interhelical side chain-side chain H-bonds [48,53]. Accordingly, the H-bonding potential of the native Thr-26, Ser-29 and Thr-37 residues located at the same helical interface of the TM segment, and/or the presence of Leu-24, Leu-27 and Leu-31 at positions **a**, **d** and the following **a** position, may indicate two alternative interfaces of self-interaction (Fig. 6A), thereby providing the core sequence with the innate capacity to form dimers and trimers in membrane environments. In order to visualize the structures of homo-dimeric sequences of L22–W39 from potential TM segments of DGKε in further detail, we applied the CHI program [17] and obtained several clusters of structures, including the two categories of models shown in Fig. 6B. In one model (Fig. 6B, I), the functional–OH groups on Thr-26 and Ser-29 side chains [53] are oriented toward the helix interaction surfaces. In the second category (Fig. 6B, II), the leucine zipper motif experiences mutual proximity within the interaction surface of the dimer, while the side chains of Thr-26 and Ser-29 are now oriented outside of this surface. The modeling is consistent with the notion that the putative TM segment of DGKε is capable of self-association into dimers – or potentially higher order oligomers – through either interhelical H-bonding and/or hydrophobic interactions. Since the CHI program input is limited to data relating to atomic van der Waals radii, and does not specifically take into account extant electrostatic or polar interactions, it would not recognize potential H-bonds between side chains of Thr-26, Ser-29 or Thr-37. However, given that the packing is already optimized in these structures, any side chain-side chain H-bonding that may arise between proximal Ser and Thr side chains would only add to dimer stability. Unlike the model peptide, L22W39-K_9, the isolated full-length protein has only a weak tendency to dimerize in the presence of the weak detergent perfluorooctanoic acid [54]. It is possible that this weak dimerization tendency is expressed in biological membranes where the protein may be concentrated in particular membrane domains.

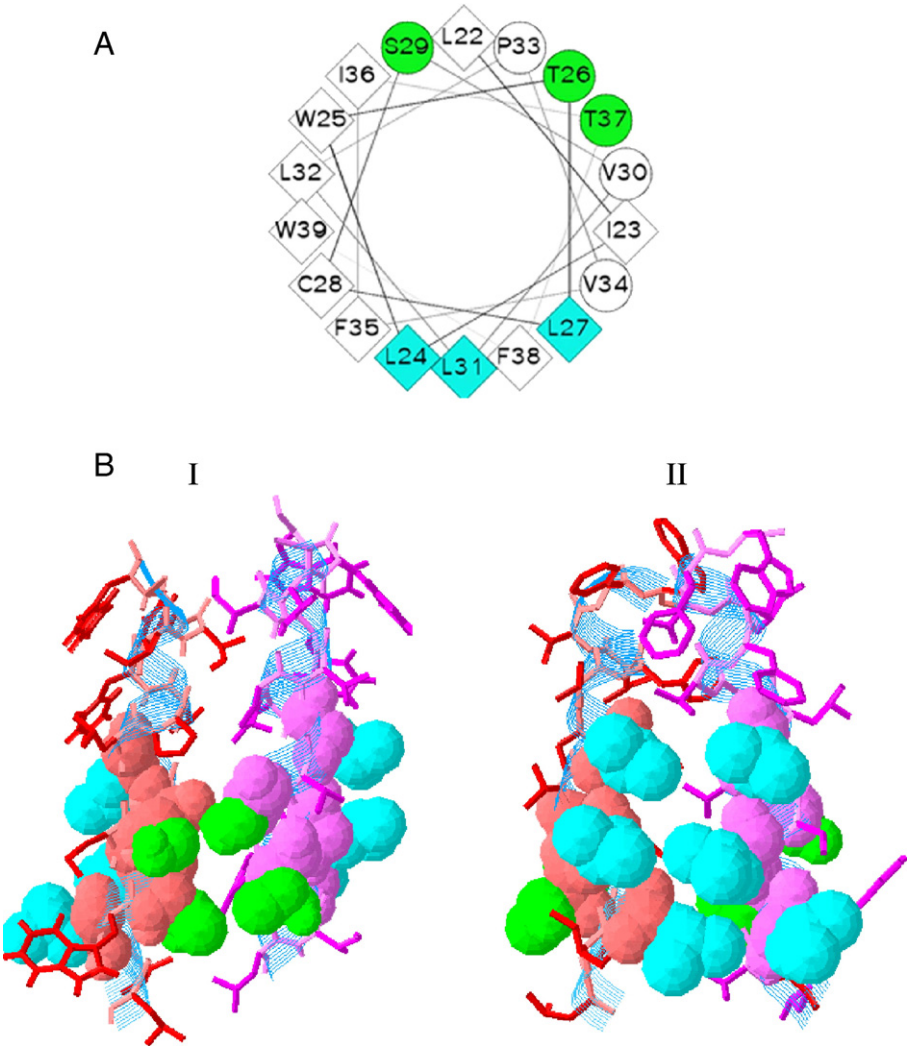

Fig. 6. (A) Helical wheel representation of the L22–W39 sequence, indicating the positioning of residues Thr-26, Ser-29, and Thr-37 on one potential interaction surface (green circles), and Leu-24, Leu-27 and Leu-31 (blue diamonds) on an opposing face. The model was generated using wheel.pl program (http://rzlab.ucr.edu/scripts/wheel/wheel.cgi) (B) Two categories of energy-minimized dimer models from the hydrophobic core L22–W39 sequence, displaying the interaction surface between the parallel helical segments. Hydroxyl-containing side chains of Thr-26 and Ser-29 are rendered in green (left, I); aliphatic side chains of interacting leucine zipper residues Leu-24, Leu-27 and Leu-31 are rendered in blue (right, II). The models were generated using the global conformational search software CHI (see Materials and methods) with idealized helices corresponding to the native peptide sequence. A dielectric constant of 1 was used in the calculations.

Other isoforms of DGK are known to be regulated by modulators. It is therefore likely, *a priori*, that there is a mechanism for turning on and off the enzymatic activity of DGKε. A putative mechanism for this could occur *via* oligomerization – in turn altering the enzymatic activity. Since the L22W39-K_9 peptide exists as stable dimers, one could hypothesize that the effects of oligomerization may be mimicked *in vivo* by association of the L22–W39 hydrophobic segment of intact DGKε. Indeed, when the peptide was added to an assay for the activity of DGKε there was significant inhibition (Fig. 4). However, since we observed a similar extent of inhibition using another isoform, DGKζ, that does not have an intrinsic hydrophobic domain, the mode of inhibition appears to be non-specific and could be the result of protein interactions with the L22W39-K_9 peptide anchored into the membrane interface. The latter mechanism of inhibition of this peptide requires further investigation.

4.3. Peptide interaction with cholesterol

An ancillary role for the hydrophobic segment is that it is responsible for the localization of DGKε to specific domains in the membrane. There is much current interest in the possible role of raft-like, cholesterol-rich domains in signal transduction processes [55]. The fact that the nature of the insertion of the peptide into a membrane is influenced by cholesterol is shown by the CD results using anionic bilayers without or with added cholesterol (Fig. 1B). In addition, our DSC experiments show that L22W39-K_9 causes an increase in the enthalpy of the SOPC transition in mixtures of SOPC and cholesterol (Fig. 5, Table 3). This effect is particularly large at 40 mol% cholesterol and suggests that the peptide can partially deplete a domain of the membrane from cholesterol. The increase in the cooperativity and enthalpy of the SOPC melting transition demonstrates that cholesterol and peptide are being removed into a separate

domain of the membrane. Being specific for polyunsaturated acyl chains is suggestive that DGKε is involved with the resynthesis of PtnIns(4,5)bisphosphate by catalyzing the phosphorylation of the diacylglycerol that is liberated by activation of PtnIns(4,5)bisphosphate-specific phospholipase C. This is because it is known that PtnIns(4,5)bisphosphate is highly enriched with arachidonic acid. There is controversy regarding the location of PtnIns(4,5)bisphosphate in membranes, but it is possible that it is co-sequestered with DGKε in a cholesterol-rich membrane domain.

5. Conclusion

We find that a peptide corresponding to the putative DGKε transmembrane segment – flanked by Lys tags – ultimately cannot leave the bulk water for attachment/insertion into erythrocyte-like outer leaflet bilayers, yet its core sequence is sufficiently hydrophobic to insert into membrane core regions when membrane attachment is promoted by electrostatic attraction to anionic lipid head groups. Our combined observations suggest that the L22W39-K_9 peptide may be only partially inserted in bilayers—an indication that full transmembrane insertion may not be occurring, and/or equilibrium processes are operative. These findings may have implications *in vivo*, where the asymmetry of bilayers is such that anionic lipids similarly occur largely on the inner (cytoplasmic) leaflet. Conceivably, the presence of Lys residues added during synthesis may dominate interactions with anionic lipids, but minimize any specific attraction to zwitterionic membrane surfaces. However, several positively-charged residues are similarly present near the ostensible TM stretch in the DGKε native TM sequence. Whether transmembrane or surface-embedded, our overall results demonstrate that the L22W39-K_9 peptide is readily capable of strong interactions with lipid membranes.

Acknowledgements

This work was supported, in part, by a grant to R.M.E. from the Canadian Natural Sciences and Engineering Research Council (NSERC 9848) and by a grant to C.M.D. from the Canadian Institutes for Health Research (CIHR). E.G. held a post-doctoral award from the CIHR Strategic Program in the Structural Biology of Membrane Proteins Linked to Disease. R.M.E. holds a Senior Investigator award from the CIHR.

References

[1] M.K. Topham, Signaling roles of diacylglycerol kinases, J. Cell. Biochem. 97 (2006) 474–484.
[2] S. Imai, M. Kai, S. Yasuda, H. Kanoh, F. Sakane, Identification and characterization of a novel human type II diacylglycerol kinase, DGK kappa, J. Biol. Chem. 280 (2005) 39870–39881.
[3] W.J. Van Blitterswijk, B. Houssa, Properties and functions of diacylglycerol kinases, Cell. Signal. 12 (2000) 595–605.
[4] F. Sakane, H. Kanoh, Molecules in focus: diacylglycerol kinase, Int. J. Biochem. Cell Biol. 29 (1997) 1139–1143.
[5] H. Kanoh, K. Yamada, F. Sakane, Diacylglycerol kinases: emerging downstream regulators in cell signaling systems, J. Biochem. (Tokyo) 131 (2002) 629–633.
[6] M.K. Topham, S.M. Prescott, Mammalian diacylglycerol kinases, a family of lipid kinases with signaling functions, J. Biol. Chem. 274 (1999) 11447–11450.
[7] N.G. Bazan, Lipid signaling in neural plasticity, brain repair, and neuroprotection, Mol. Neurobiol. 32 (2005) 89–103.
[8] A. Musto, N.G. Bazan, Diacylglycerol kinase epsilon modulates rapid kindling epileptogenesis, Epilepsia 47 (2006) 267–276.
[9] E.B. Rodriguez de Turco, W. Tang, M.K. Topham, F. Sakane, V.L. Marcheselli, C. Chen, A. Taketomi, S.M. Prescott, N.G. Bazan, Diacylglycerol kinase epsilon regulates seizure susceptibility and long-term potentiation through arachidonoyl-inositol lipid signaling, Proc. Natl. Acad. Sci. U. S. A. 98 (2001) 4740–4745.
[10] W. Tang, M. Bunting, G.A. Zimmerman, T.M. McIntyre, S.M. Prescott, Molecular cloning of a novel human diacylglycerol kinase highly selective for arachidonate-containing substrates, J. Biol. Chem. 271 (1996) 10237–10241.
[11] S. Thirugnanam, M.K. Topham, R.M. Epand, Physiological implications of the contrasting modulation of the activities of the ε and ζ Isoforms of diacylglycerol kinase, Biochemistry 40 (2001) 10607–10613.
[12] F.C. Gomez-Merino, C.A. Brearley, M. Ornatowska, M.E.F. Abdel-Haliem, M.I. Zanor, B. Mueller-Roeber, AtDGK2, a novel diacylglycerol kinase from *Arabidopsis thaliana*, phosphorylates 1-Stearoyl-2-arachidonoyl-*sn*-glycerol and 1,2-Dioleoyl-*sn*-glycerol and exhibits cold-inducible gene expression, J. Biol. Chem. 279 (2004) 8230–8241.
[13] C. Horie, H. Suzuki, M. Sakaguchi, K. Mihara, Characterization of signal that directs C-tail-anchored proteins to mammalian mitochondrial outer membrane, Mol. Biol. Cell 13 (2002) 1615–1625.
[14] A.W. Partridge, R.A. Melnyk, D. Yang, J.U. Bowie, C.M. Deber, A transmembrane segment mimic derived from *Escherichia coli* diacylglycerol kinase inhibits protein activity, J. Biol. Chem. 278 (2003) 22056.
[15] C.M. Deber, C. Wang, L.P. Liu, A.S. Prior, S. Agrawal, B.L. Muskat, A.J. Cuticchia, TM Finder: a prediction program for transmembrane protein segments using a combination of hydrophobicity and nonpolar phase helicity scales, Protein Sci. 10 (2001) 212–219.
[16] R. Zidovetzki, B. Rost, D.L. Armstrong, I. Pecht, Transmembrane domains in the functions of Fc receptors, Biophys. Chem. 100 (2003) 555–575.
[17] P.D. Adams, D.M. Engelman, A.T. Brunger, Improved prediction for the structure of the dimeric transmembrane domain of glycophorin A obtained through global searching, Proteins 26 (1996) 257–261.
[18] M. Stark, L.P. Liu, C.M. Deber, Cationic hydrophobic peptides with antimicrobial activity, Antimicrob. Agents Chemother. 46 (2002) 3585–3590.
[19] E. Glukhov, M. Stark, L.L. Burrows, C.M. Deber, Basis for selectivity of cationic antimicrobial peptides for bacterial versus mammalian membranes, J. Biol. Chem. 280 (2005) 33960–33967.
[20] D.B. Masters, C.T. Griggs, C.B. Berde, High sensitivity quantification of RNA from gels and autoradiograms with affordable optical scanning, BioTechniques 12 (1992) 902–911.
[21] L.P. Liu, C.M. Deber, Anionic phospholipids modulate peptide insertion into membranes, Biochemistry 36 (1997) 5476–5482.
[22] L.P. Liu, C.M. Deber, Uncoupling hydrophobicity and helicity in transmembrane segments. Alpha-helical propensities of the amino acids in non-polar environments, J. Biol. Chem. 273 (1998) 23645–23648.
[23] Y.H. Chen, J.T. Yang, K.H. Chau, Determination of the helix and beta form of proteins in aqueous solution by circular dichroism, Biochemistry 13 (1974) 3350–3359.
[24] R.A. Melnyk, A.W. Partridge, C.M. Deber, Transmembrane domain mediated self-assembly of major coat protein subunits from Ff bacteriophage, J. Mol. Biol. 315 (2002) 63–72.
[25] G. Privalov, V. Kavina, E. Freire, P.L. Privalov, Precise scanning calorimeter for studying thermal properties of biological macromolecules in dilute solution, Anal. Biochem. 232 (1995) 79–85.
[26] P. Ducarme, M. Rahman, R. Brasseur, IMPALA: a simple restraint field to simulate the biological membrane in molecular structure studies, Proteins 30 (1998) 357–371.
[27] M. Cserzo, E. Wallin, I. Simon, G. von Heijne, A. Elofsson, Prediction of

transmembrane alpha-helices in prokaryotic membrane proteins: the dense alignment surface method, Protein Eng. 10 (1997) 673–676.
[28] A. Saez-Cirion, J.L. Arrondo, M.J. Gomara, M. Lorizate, I. Iloro, G. Melikyan, J.L. Nieva, Structural and functional roles of HIV-1 gp41 pretransmembrane sequence segmentation, Biophys. J. 85 (2003) 3769–3780.
[29] G.B. Melikyan, S. Lin, M.G. Roth, F.S. Cohen, Amino acid sequence requirements of the transmembrane and cytoplasmic domains of influenza virus hemagglutinin for viable membrane fusion, Mol. Biol. Cell 10 (1999) 1821–1836.
[30] G. Gafvelin, M. Sakaguchi, H. Andersson, H.G. von, Topological rules for membrane protein assembly in eukaryotic cells, J. Biol. Chem. 272 (1997) 6119–6127.
[31] R.A. Melnyk, A.W. Partridge, C.M. Deber, Retention of native-like oligomerization states in transmembrane segment peptides: application to the *Escherichia coli* aspartate receptor, Biochemistry 40 (2001) 11106–11113.
[32] C. Wang, C.M. Deber, Peptide mimics of the M13 coat protein transmembrane segment. Retention of helix–helix interaction motifs, J. Biol. Chem. 275 (2000) 16155–16159.
[33] G.A. Caputo, E. London, Cumulative effects of amino acid substitutions and hydrophobic mismatch upon the transmembrane stability and conformation of hydrophobic alpha-helices, Biochemistry 42 (2003) 3275–3285.
[34] J.A. Op den Kamp, Lipid asymmetry in membranes, Annu. Rev. Biochem. 48 (1979) 47–71.
[35] A.S. Ladokhin, S. Jayasinghe, S.H. White, How to measure and analyze tryptophan fluorescence in membranes properly, and why bother? Anal. Biochem. 285 (2000) 235–245.
[36] B.D. Adair, D.M. Engelman, Glycophorin A helical transmembrane domains dimerize in phospholipid bilayers: a resonance energy transfer study, Biochemistry 33 (1994) 5539–5544.
[37] M. You, E. Li, W.C. Wimley, K. Hristova, Forster resonance energy transfer in liposomes: measurements of transmembrane helix dimerization in the native bilayer environment, Anal. Biochem. 340 (2005) 154–164.
[38] W. Veatch, L. Stryer, The dimeric nature of the gramicidin A transmembrane channel: conductance and fluorescence energy transfer studies of hybrid channels, J. Mol. Biol. 113 (1977) 89–102.
[39] Y. Goto, Y. Hagihara, Mechanism of the conformational transition of melittin, Biochemistry 31 (1992) 732–738.
[40] R.M. Epand, Do proteins facilitate the formation of cholesterol-rich domains? Biochim. Biophys. Acta 1666 (2004) 227–238.
[41] R.M. Epand, Detecting the presence of membrane domains using DSC, Biophys. Chem. 126 (2007) 197–200.
[42] C.R. Loomis, G.G. Shipley, D.M. Small, The phase behavior of hydrated cholesterol, J. Lipid Res. 20 (1979) 525–535.
[43] R.M. Epand, D. Bach, N. Borochov, E. Wachtel, Cholesterol crystalline polymorphism and the solubility of cholesterol in phosphatidylserine, Biophys. J. 78 (2000) 866–873.
[44] R.M. Epand, B.G. Sayer, R.F. Epand, Peptide-induced formation of cholesterol-rich domains, Biochemistry 42 (2003) 14677–14689.
[45] F. Porcelli, B. Bethany, D.K. Lee, K.J. Hallock, A. Ramamoorthy, G. Veglia, Structure and orientation of pardaxin determined by NMR experiments in model membranes, J. Biol. Chem. 279 (2004) 45815–45823.
[46] R.F. Epand, A. Ramamoorthy, R.M. Epand, Membrane lipid composition and the interaction of pardaxin: the role of cholesterol, Prot. Peptide Letters 13 (2006) 1–5.
[47] C. Choma, H. Gratkowski, J.D. Lear, W.F. DeGrado, Asparagine-mediated self-association of a model transmembrane helix, Nat. Struct. Biol. 7 (2000) 161–166.
[48] F.X. Zhou, M.J. Cocco, W.P. Russ, A.T. Brunger, D.M. Engelman, Interhelical hydrogen bonding drives strong interactions in membrane proteins, Nat. Struct. Biol. 7 (2000) 154–160.
[49] J.D. Lear, A.L. Stouffer, H. Gratkowski, V. Nanda, W.F. DeGrado, Association of a model transmembrane peptide containing gly in a heptad sequence motif, Biophys. J. 87 (2004) 3421–3429.
[50] R. Gurezka, R. Laage, B. Brosig, D. Langosch, A heptad motif of leucine residues found in membrane proteins can drive self-assembly of artificial transmembrane segments, J. Biol. Chem. 274 (1999) 9265–9270.
[51] N. Asthana, S.P. Yadav, J.K. Ghosh, Dissection of antibacterial and toxic activity of melittin: a leucine zipper motif plays a crucial role in determining its hemolytic activity but not antibacterial activity, J. Biol. Chem. 279 (2004) 55042–55050.
[52] A. Rath, R.M. Johnson, C.M. Deber, Peptides as transmembrane segments: decrypting the determinants for helix–helix interactions in membrane proteins, Biopolymers 88 (2007) 217–232.
[53] J.P. Dawson, J.S. Weinger, D.M. Engelman, Motifs of serine and threonine can drive association of transmembrane helices, J Mol. Biol. 316 (2002) 799–805.
[54] A.O. Dicu, M.K. Topham, L. Ottaway, R.M. Epand, Role of the hydrophobic segment of diacylglycerol kinase epsilon, Biochemistry 46 (2007) 6109–6117.
[55] K. Simons, D. Toomre, Lipid rafts and signal transduction, Nat. Rev., Mol. Cell Biol. 1 (2000) 31–39.